

Gluon excitations in $t\bar{t}$ production at hadron colliders

R. Barceló, A. Carmona, M. Masip, J. Santiago

*CAFPE and Departamento de Física Teórica y del Cosmos
Universidad de Granada, E-18071, Granada, Spain*

rbarcelo@ugr.es, adrian@ugr.es, masip@ugr.es, jsantiago@ugr.es

Abstract

We argue that a relatively light massive gluon with mass $\lesssim 1$ TeV, small purely axial couplings to light quarks and sizable vector and axial couplings to the top quark can reproduce the large forward-backward asymmetry observed at the Tevatron without conflicting with the $t\bar{t}$ and the dijet invariant mass distributions measured at the Tevatron and the LHC. We show that realistic Higgsless models with warped extra dimensions naturally fulfil all the necessary ingredients to realize this scenario. While current data is unable to discover or exclude these heavy gluons with masses ≈ 850 GeV, they should be observed at the (7 TeV) LHC with a luminosity $\gtrsim 300$ pb $^{-1}$.

1 Introduction

The standard model (SM) does not *explain* the difference between the electroweak (EW) and the Planck scales ($M_{EW}^2 \approx 10^{-32} M_{Planck}^2$). The large value of the top mass makes it plausible that any new physics responsible for this difference would show up in top physics. Thus a detailed study of top properties is one of the main goals of the Tevatron and the LHC. In fact, Tevatron experiments have already observed a significant anomaly in the forward-backward asymmetry $A^{t\bar{t}}$ in $t\bar{t}$ production [1, 2, 3], an anomaly that is not present in the total cross section (*i.e.* integrated over all angles). It is not easy to explain this anomaly with current Tevatron and LHC data on dijets and top-pair production. New heavy color octet gauge bosons with axial couplings to the SM quarks, axigluons, have been proposed as possible candidates [4, 5, 7] (see also [6] for a model independent discussion). The reason, that we review below, is that axial couplings contribute maximally to the asymmetry but cancel to leading order in the total cross section.

In this article we point out a region of parameter space of these color octets that has been overlooked in the past.¹ It corresponds to relatively light $m_G \lesssim 1$ TeV gluons with small axial couplings to the light quarks and order one axial and vector couplings to the top quark. As we will show, the axial nature of the couplings to light quarks and the mass of the new gluon are enough to hide it from Tevatron data on the total cross section and the $t\bar{t}$ invariant mass distribution ($M_{t\bar{t}}$) while agreeing with the observed asymmetry. At the LHC the small couplings to the light quarks (and the zero coupling to gluons) makes the heavy gluon invisible in dijet data, whereas the luminosity of the 2010 LHC run is not enough to make it visible in $t\bar{t}$ data. It should however show up clearly in the data to be collected during the 2011 run.

Interestingly enough, Higgsless models with warped extra dimensions [8, 9] naturally realize the scenario we have just discussed. In these models there are massive copies, the Kaluza-Klein (KK) excitations, of the SM gauge bosons, including the gluon, with masses bound from below by EW precision tests to be $M_G \gtrsim 0.7$ TeV and from above from the fact that the KK excitations of the EW gauge bosons have to unitarize longitudinal gauge boson scattering, $m_G \lesssim 1$ TeV (the masses of the KK excitations of the gluons and the EW bosons are of the same order). At the same time it is natural that the left and right handed components of the SM fermions are localized at different points of the extra dimension, which means that their couplings to the KK gluons are in general different. Therefore, KK gluons

¹A related discussion, with emphasis on fourth-generation quark production in the context of models of strong EW symmetry breaking can be found in [7].

will have both vector and axial-vector couplings to fermions:

$$g_V^f = \frac{g_R^f + g_L^f}{2}, \quad g_A^f = \frac{g_R^f - g_L^f}{2}. \quad (1)$$

As we will see below, constraints on these models from EW precision data tend to require the couplings of the light quarks to the KK gluon to be small and mainly axial, as it is also preferred by top data. Such axigluons have another *unusual* feature, namely, they do not decay into massless gluons. This can be easily understood from the orthogonality of their wave functions: the overlap between an initial massive mode and the two final (delocalized) gluons adds always to zero. The KK excitations are then far from being massive replicas of the standard zero mode, as often assumed in collider searches. Here we study under what conditions they are consistent with the data on $t\bar{t}$ production at the Tevatron and with LHC data.

The outline of the paper is as follows. In the section 2 we review the effect of new heavy gluons with vector and axial couplings on Tevatron data. In section 3 we describe the relevant features of realistic Higgsless models and how they naturally realize new axigluons compatible with Tevatron data. Section 4 is devoted to the implication of realistic models at the LHC and finally we conclude in section 5.

2 Vector and axial-vector gluons at the Tevatron

Before considering a more motivated model, we review the impact that a massive gluon G may have on $t\bar{t}$ physics in the simplest cases (for a related discussion see [4, 5, 7]). We will focus on $M_{t\bar{t}}$ and $A^{t\bar{t}}$, two observables that have been measured at the Tevatron with an integrated luminosity up to 5.3 fb^{-1} . We use the parton level asymmetry in the $t\bar{t}$ rest frame that has been measured to be [3]

$$A^{t\bar{t}} = 0.474 \pm 0.114. \quad (2)$$

We consider two different options according to the coupling of G to the light quarks:

- Coupling to vector currents (*case V*):

$$g_V^q = g_R^q = g_L^q; \quad g_A^q = 0. \quad (3)$$

- Coupling to axial currents (*case A*):

$$g_A^q = g_R^q = -g_L^q; \quad g_V^q = 0. \quad (4)$$

For the top quark we will simply assume

$$g_R^t \geq g_L^t > 0. \quad (5)$$

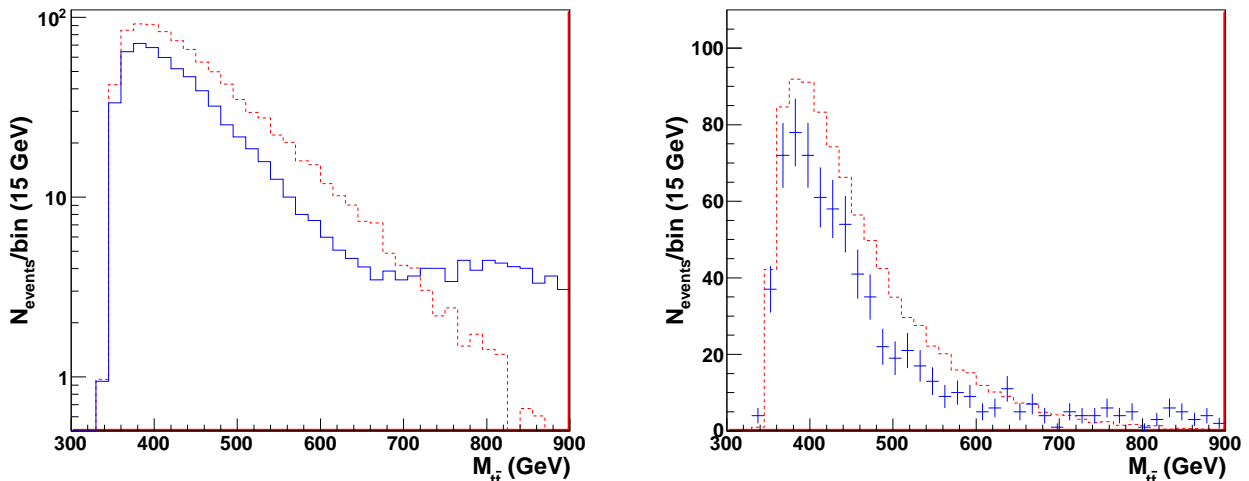


Figure 1: $M_{t\bar{t}}$ distribution at the Tevatron in the SM (dashes) and in model V (solid) for a luminosity of 5.3 fb^{-1} and $g_V^q = +0.2$. On the left we plot the average number of events expected in each case, and on the right a particular Monte Carlo simulation. The errors shown are statistical only.

We have implemented the model in MADGRAPH/MADEVENT v4 [10], used PYTHIA [11] for hadronization and showering and PGS4 [12] for detector simulation. In Fig. 1 we plot $M_{t\bar{t}}$ distribution for *case V* with $(g_V^q = 0.2g, g_A^q = 0)$, $(g_R^t = 6g, g_L^t = 0.2g)$ and a mass $M_G = 850 \text{ GeV}$. For these couplings the gluon width is $\Gamma_G \approx 0.32M_G$. We have taken an integrated luminosity of 5.3 fb^{-1} and the cuts/acceptances described in [3] (we have normalized our samples so that our SM prediction agrees with the background-subtracted data of [3]). The 682 semileptonic $t\bar{t}$ pairs given by this model (see Fig. 1-*left*) result from the destructive interference of the standard $[\approx g^2/\hat{s}]$ and the massive-gluon $[\approx 0.2g \cdot 6g/(-M^2)]$ amplitudes. We obtain a 30% reduction for $M_{t\bar{t}} < M_G - \Gamma_G$ and an excess at higher invariant masses with respect to the SM. The distribution does not show a clear peak, but the change in the *slope* at $M_{t\bar{t}} \approx 650 \text{ GeV}$ would have been apparent in the data. Taking the opposite sign for the light-quark vector coupling $(g_V^q = -0.2g, g_A^q = 0)$ the situation is similar, although the interference is now constructive at low values of $M_{t\bar{t}}$.

In these models the forward-backward asymmetry will appear only at next-to-leading order, since $A_G^{t\bar{t}} \propto -g_A^q g_A^t = 0$ (see for example [4]). In particular, the interference of the

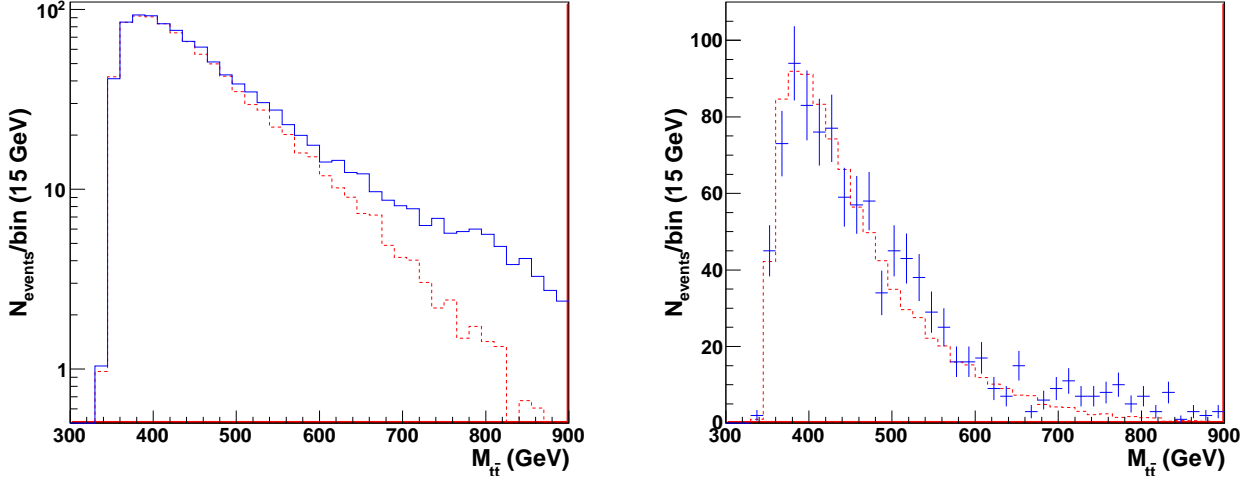


Figure 2: $M_{t\bar{t}}$ distribution at the Tevatron in the SM (dashes) and in model A (solid) for a luminosity of 5.3 fb^{-1} and $g_A = -0.2$. On the left we plot the average number of events expected in each case, and on the right a particular Montecarlo simulation. The errors shown are statistical only.

tree-level and the one-loop box amplitudes will provide the standard contribution, of order $A_{NLO}^{t\bar{t}} \approx 0.09$ at high invariant masses as estimated in [3] using MCFM [13]. An analogous interference between the massive gluon and the box diagrams will also contribute to the asymmetry. At $M_{t\bar{t}} \ll M_G$ we estimate (see also [14])

$$A_{V-NLO}^{t\bar{t}} \approx A_{NLO}^{t\bar{t}} \times \frac{M_{t\bar{t}}^2}{-M_G^2} \frac{g_V^q g_V^t}{g^2}, \quad (6)$$

implying an additional contribution of order $A_{V-NLO}^{t\bar{t}} \approx \mp 0.04$ for $g_V^q = \pm 0.2 g$. Therefore, the total value seems in this *case V* very far (over 3σ) from the asymmetry deduced from the Tevatron data.

Case A, with a purely axial-vector coupling to the light quarks, is completely different. Both $q_L \bar{q}_L \rightarrow t\bar{t}$ and $q_R \bar{q}_R \rightarrow t\bar{t}$ parton-level cross sections will have large contributions from the interference. However, since their couplings are opposite ($g_L^q = -g_R^q$), it will be constructive in the first process and destructive in the second one, and both effects tend to cancel each other. Up to invariant masses $M_{t\bar{t}} \approx M_G - \Gamma_G$ where the resonant contribution becomes important, the number of $t\bar{t}$ events and their $M_{t\bar{t}}$ distribution will be very close to the one in the standard model. Note that the top couplings do not need to be purely axial for this to happen. The region around the peak will be hidden by the low statistics if M_G is large enough. In Fig. 2 we plot *case A* with $(g_A^q = -0.2 g, g_V^q = 0)$, $(g_R^t = 6 g, g_L^t = 0.2 g)$,

$M_G = 850$ GeV and $\Gamma_G = 0.32M_G$ GeV. After cuts we obtain 1042 $t\bar{t}$ pairs, a number only 12% higher than the one expected in the standard model. At $M_{t\bar{t}} \approx 600$ GeV the distribution exhibits a change in the slope, but the region where the differences are important (around 750 GeV) is of little statistical significance (see a particular Montecarlo simulation in Fig. 2–*right*). Notice that in this model the peak at $M_{t\bar{t}} = 850 \pm 272$ GeV is practically nonexistent, so it would be challenging to exclude it at the Tevatron even with an increased luminosity.

In contrast to the case with vector couplings to the light quarks, $A_G^{t\bar{t}}$ is in *case A* large: the total number of events does not change, but there is a large forward excess that coincides with the backward deficit. In the $t\bar{t}$ rest frame we obtain

$$A_G^{t\bar{t}} \approx \begin{cases} 0.07 & M_{t\bar{t}} < 450 \text{ GeV}; \\ 0.20 & M_{t\bar{t}} > 450 \text{ GeV}. \end{cases} \quad (7)$$

Therefore, *case A* provides a promising framework for model building. Such a light axigluon could in principle be strongly constrained by flavor data. We show in the next section that Higgsless models with warped extra dimensions naturally realize the framework we have just described here. In such models one can implement flavor symmetries that keep these flavor constraints under control [15]. Also note that the couplings of the (t_L, b_L) doublet with the axigluon do not need to be too large in order to generate a sizable $A^{t\bar{t}}$ thus further reducing constraints from B physics [16].

3 Axigluons in a realistic Higgsless model

We consider the realistic warped Higgsless model proposed in [9] in which the EW symmetry is broken via boundary conditions. This can be understood as a limit with $\langle H \rangle \rightarrow \infty$ that forces the W, Z wave functions to vanish at the IR brane keeping their masses finite, while the physical (4dim) Higgs decouples. The Z and W bosons become then *anomalous* KK modes, much lighter than higher excitations and with a flatter wave function along the extra dimension. The model and its EW constraints are described in some detail in the appendix, here we just emphasize the most relevant features for $t\bar{t}$ production.

- (i) The light quarks are almost flat in the extra dimension to ensure a small coupling to the gauge KK modes. The LH (RH) light quarks have a slight preference for localization towards the IR (UV) brane that naturally makes $g_L \approx -g_R \approx 0.2 - 0.3g$. Thus the coupling is naturally small, almost purely axial and negative.
- (ii) Both components of the top (LH and RH) are localized towards the IR brane. The localization is stronger for the RH component, resulting in large couplings to the KK

gluon that are neither purely vector or purely axial, but with a positive and sizable axial component.

- (iii) The massive KK excitations of the EW gauge bosons unitarize WW scattering. This forces the gauge resonances (including the gluon) to have a mass below 1 TeV.

These features imply that Higgsless models naturally realize the light axigluon that we discussed in the previous section. Also, the first two points guarantee that the axial couplings of the light quarks and the top have opposite signs, thus giving a positive contribution to $A^{t\bar{t}}$ as observed at the Tevatron. The relatively large axial coupling of the top and light KK gluon mass make it possible to generate a sizable asymmetry without the need of large axial couplings for the light quarks. We find remarkable that all these features are entirely imposed by constraints from EW precision data and have nothing to do with top data.

The original model proposed in [9] corresponds to a first gluon excitation with a mass $M_G = 714$ GeV and the following couplings

$$\begin{aligned} g_R^q &= g_R^b = -0.31 g, & g_L^q &= +0.17 g, \\ g_R^t &= +2.27 g, & g_L^t &= g_L^b = +1.93 g, \end{aligned} \quad (8)$$

resulting in a total width $\Gamma_G = 0.13 M_G$. In Fig. 3–*left* we plot the invariant mass distribution for this model using again the luminosity (5.3 fb^{-1}) and the cuts described in [3]. The total number of $t\bar{t}$ pairs is almost a 60% higher than in the SM. In addition, the 275 events between 650 and 750 GeV form a clear peak that should have been observed in the analysis of the Tevatron data.

We show that with a minimal variation this model, while still consistent with EW data, improves the agreement with Tevatron data. The KK gluon mass is increased to 850 GeV by slightly changing the value of the IR scale $1/R' = 340$ GeV (the corresponding value of the UV scale is $1/R \approx 2.9 \times 10^{10}$ GeV, see appendix for the details). We also optimize the localization of the different quarks (while still being consistent with EW precision tests) so that the new couplings are given by

$$\begin{aligned} g_R^q &= g_R^b = -0.25 g, & g_L^q &= +0.20 g, \\ g_R^t &= +4.00 g, & g_L^t &= g_L^b = +1.00 g, \end{aligned} \quad (9)$$

With this choice of parameters, the resonance has a width $\Gamma_G = 0.17 M_G$. We show in Fig. 3–*right* the invariant-mass distribution of the 1113 $t\bar{t}$ pairs that survive the cuts. At $M_{t\bar{t}} < 600$ GeV the model gives a 8% excess respect to the SM value, whereas at higher invariant masses we obtain 197 events versus 80 within the SM. This excess, together with

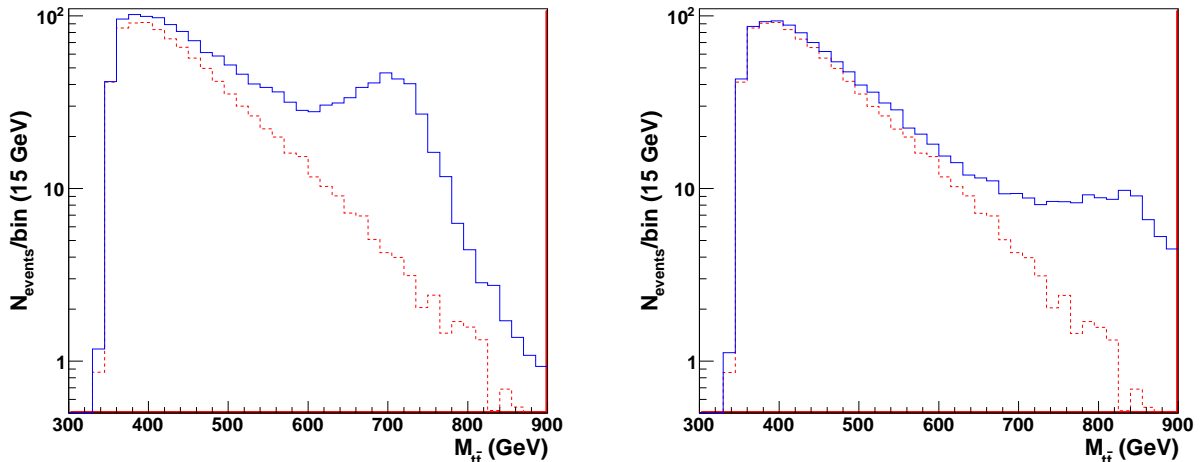


Figure 3: $M_{t\bar{t}}$ distribution at the Tevatron for Higgsless models. Left panel: original Higgsless model of Eq. (8); right panel: modified Higgsless model Eq. (9). In both cases the contribution in the Higgsless models is shown in solid while the SM only contribution is shown in dashed. We have considered a luminosity of 5.3 fb^{-1} .

the change in slope makes it likely that the model should have been seen in the Tevatron data, although only a detailed statistical analysis could state the confidence of the exclusion. Nevertheless it is clear that the slightly higher mass, the reduction in the vector component of the light-quark couplings, the enhancement of the top couplings and the increased width all go in the correct direction to hide the KK gluon in the invariant-mass distributions while increasing the agreement in the forward-backward asymmetry. The asymmetry for the original Higgsless model is very small whereas we find for the modified model

$$A_{\#}^{t\bar{t}} \text{ mod} \approx \begin{cases} 0.04 & M_{t\bar{t}} < 450 \text{ GeV}; \\ 0.16 & M_{t\bar{t}} > 450 \text{ GeV}. \end{cases} \quad (10)$$

Adding the standard NLO contribution, of order $A_{NLO}^{t\bar{t}} \approx 0.09$ for $M_{t\bar{t}} > 450 \text{ GeV}$, we obtain in the modified model a total asymmetry less than 2σ away from the measured value.

The model we have just presented improves the agreement with the observed asymmetry, although still at the price of making the model likely visible in Tevatron data on the $t\bar{t}$ invariant-mass distribution. The crucial point is that these models provide in a natural way (all features are enforced by EW data, completely unrelated to the top physics we are discussing) a framework that realizes a light axigluon with the right couplings. Small variations of the model can easily further improve the agreement with the observed asymmetry without conflict with current data on the invariant-mass distribution. In particular, it is

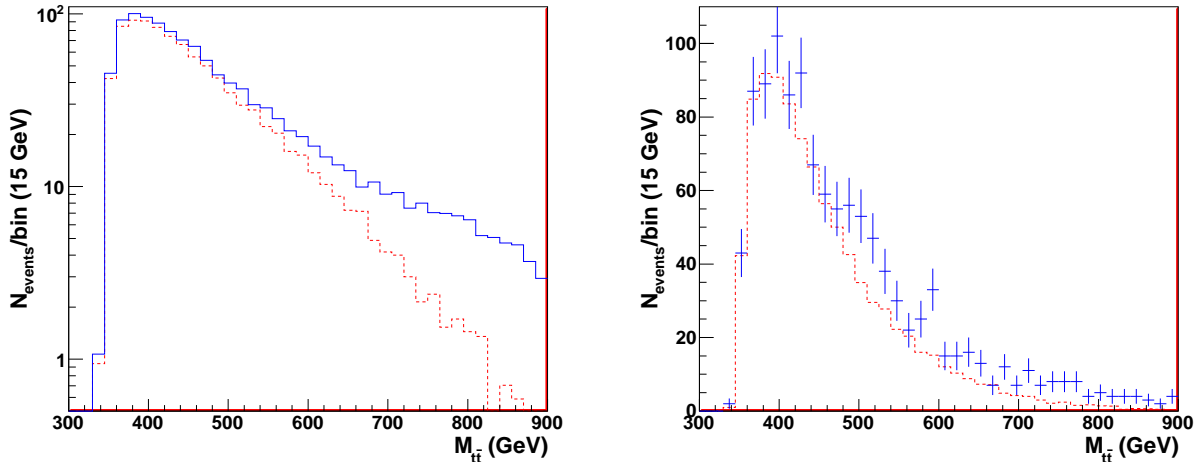


Figure 4: $M_{t\bar{t}}$ distribution at the Tevatron in the SM (dashes) and in the modified Higgsless model (solid) for a luminosity of 5.3 fb^{-1} . On the right we plot a particular Montecarlo simulation. The errors shown are statistical only.

clear that making the RH top coupling a bit larger will increase the asymmetry and the width of the gluon resonance, thus suppressing the peak structure in the tail of the invariant mass distribution.

As an example, we have taken the following values of the couplings, with the same KK gluon mass,

$$\begin{aligned} g_R^a &= g_R^b = -0.25 g, & g_L^a &= +0.20 g, \\ g_R^t &= +6.00 g, & g_L^t &= g_L^b = +0.20 g. \end{aligned} \quad (11)$$

resulting in a width $\Gamma_G = 0.32M_G$. This model is very similar to model A in the introduction. We show in Fig. 4 the $t\bar{t}$ invariant mass distribution after cuts for the model and the SM contribution (left panel) and a particular MonteCarlo simulation with the collected luminosity to show that the differences are not statistically significant (right panel). The asymmetry is increased in this case to

$$A_{\cancel{H}}^{t\bar{t}} \approx \begin{cases} 0.07 & M_{t\bar{t}} < 450 \text{ GeV}; \\ 0.23 & M_{t\bar{t}} > 450 \text{ GeV}. \end{cases} \quad (12)$$

leaving the total asymmetry just 1.4σ below the observed value. Just like for model A in the introduction, the cross section for $M_{t\bar{t}} < 600 \text{ GeV}$ is a bit above the SM expectation (8%). This fact (that could influence the normalization of the experimental data) together with the absence of any feature (peak) along the tail would make the model difficult to see at the Tevatron.

4 Invariant mass distribution at the LHC

We have seen that warped Higgsless models provide a framework with all the required ingredients to explain the observed $A^{t\bar{t}}$ without conflicting with Tevatron data on the total cross section. Even with the low integrated luminosity collected by LHC in the 2010 run, analyses of dijet and $t\bar{t}$ data are beginning to probe the parameter space of many models proposed to explain the Tevatron asymmetry. In this section we show that the Higgsless motivated model of Eq. (11) cannot be seen with the current luminosity but should be either discovered or excluded with 2011 data. Also the small couplings to light quarks and vanishing couplings to SM gluons make the model invisible in the dijet sample.

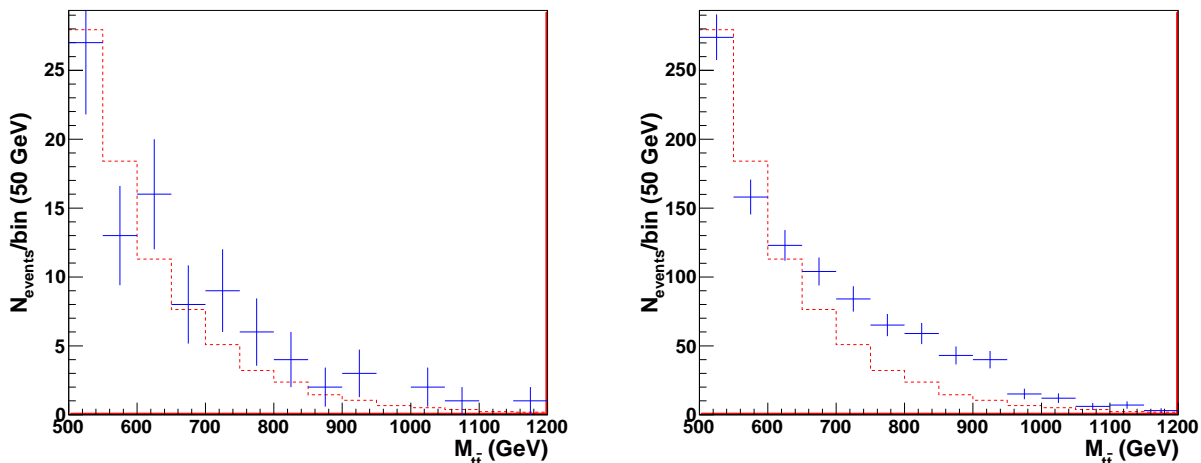


Figure 5: $M_{t\bar{t}}$ distribution at the LHC in the SM (dashes) and in the Higgsless motivated model of Eq. (11) (solid) for a luminosity of 36 pb^{-1} (left) and 360 pb^{-1} (right). We show particular Montecarlo simulations corresponding to the simulated luminosity. Errors shown are statistical only.

We have considered a luminosity of 36 pb^{-1} at 7 TeV. In Fig. 5–left we plot the number of events after cuts per 50 GeV bin, as described in [17], for a particular Montecarlo simulation. We obtain 24 events in the 700-1000 GeV interval for our model versus 14 events for the SM. It is apparent that the low number of events makes *invisible* the peak around $M_{t\bar{t}} = 850$ GeV. Increasing the luminosity by a factor of 10 (right panel of the figure) we obtain 306 events in the 700-1000 GeV interval (versus just 138 in the SM). The excess in the signal should be enough to provide evidence for this type of gluon excitation.

As for dijet signals, the particular features of the model under consideration make it completely invisible. We show in Fig. 6 the leading dijet production mechanism through

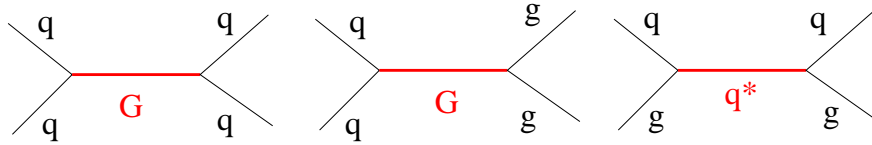


Figure 6: Dijet processes through KK gluons (G) and quarks (q^*). Possible t and u channel contributions are not explicitly shown. The first amplitude is suppressed by the couplings to the light quarks, whereas the other two vanish due to the orthogonality of the wave functions.

massive gluon or quark resonances. The first diagram has the suppression of the couplings to the light quarks giving a branching ratio $BR(G \rightarrow q\bar{q}) \approx 2\%$. The ATLAS analysis [18] is sensitive to a cross section of the order of a 10% of the one expected for an axigluon of mass 850 GeV with $g_A = g$ to the light quarks, well above the suppression in our model. To confirm this expectation we have simulated dijet events at the LHC and found that less than around 0.5% of the events pass the cuts in the analysis of [18] (the extra suppression is due to the dominant gluon initiated processes that remain unchanged in our model). The second and third diagrams of Fig. 6 exactly vanish in our model due to the orthogonality of the zero and the massive wave functions.

5 Summary and discussion

A strong forward-backward asymmetry may seem a very unexpected feature in the usual scenarios for physics beyond the standard model. We have argued that realistic Higgsless models with warped extra dimensions naturally provide a general framework to generate such an asymmetry. In these models one expects massive gluon excitations strongly coupled to the top quark, with much smaller couplings to light quarks and gluons (as required by dijet searches at the LHC [18]). In addition, the vector coupling of the light quarks may be weaker than the axial-vector one ($g_V^q \ll g_A^q$), which suppresses anomalies in the $t\bar{t}$ invariant mass distribution while introducing forward-backward asymmetry (note that the couplings of the top quark do not need to be mostly axial to cancel the largest contributions to the total cross section). It is remarkable that all these features are imposed on Higgsless models by EW physics rather than top physics. In particular, EW constraints force the new physics contribution to $A_{t\bar{t}}$ to be positive, as experimentally observed.

We have shown that, while the original Higgsless model is excluded by Tevatron top data, a slight modification can increase the agreement with the $t\bar{t}$ asymmetry while making it (barely) consistent with the invariant-mass distribution. This has motivated us to propose

a Higgsless inspired model that is compatible with Tevatron data.

The model consists of a massive gluon of ≈ 850 GeV with mostly axial-vector couplings to the light quarks and both vector and axial-vector couplings to the top quark. We show that the Tevatron does not have enough energy to *see* a peak at $M_{t\bar{t}} \approx M_G$, whereas the change in the slope of the $M_{t\bar{t}}$ distribution at $M_{t\bar{t}} \approx 650$ GeV is of little statistical significance. We have also shown that the LHC has enough energy to reach the resonance but not yet enough integrated luminosity. We have seen that about 10 times more luminosity than the current 36 pb^{-1} should be enough to probe the model. Finally, the suppressed coupling to light quarks makes the new resonance virtually invisible in dijet data.

There are some aspects of Higgsless models that we have not fully explored here and deserve further investigation. For instance, the optimal values of the couplings for the third generation quarks in the minimal realistic set-up presented in [9, 15] bring the disagreement with the observed asymmetry down to $\approx 2\sigma$, but it seems difficult to improve this results in the context of these minimal models. Furthermore, even with such modifications, there is still a small peak that might be observable in the Tevatron data. It would be interesting to see if simple modifications, for instance in the gravitational background, could allow for a larger axial top coupling to improve the agreement with $A^{t\bar{t}}$ and the invariant mass distribution. We have shown that such a modification improves the level of agreement with current data on the total cross section and the asymmetry at the Tevatron while making it invisible at the LHC (both in $t\bar{t}$ and dijet data). Also, we have not included the effect of fermion KK excitations. Some of them can be relatively light and influence the collider implications of the KK gluon. It would be interesting to see in which direction these modifications go and the interplay between KK gluon searches and fermion KK searches at the LHC (see [19] for an example of these effects). In principle, the new quarks would increase the width of the resonance and decrease the branching ratio into top pairs thus making the peak even more difficult to detect at the Tevatron.

A Details of the Higgsless Model

Let us briefly review the most relevant features of a realistic Higgsless Model with flavor protection. Full details can be found in [9, 15]. The model lives in 5D with a metric

$$ds^2 = \left(\frac{R}{z}\right)^2 [dx^2 - dz^2], \quad (13)$$

where the extra dimension is bounded $R \leq z \leq R'$ by the UV and IR branes, respectively. The bulk gauge symmetry is $SU(3)_C \times SU(2)_L \times SU(2)_R \times U(1)_X$, broken by boundary

conditions to $SU(3)_C \times U(1)_Q$. We focus on the quark sector. The first two generations live in $(2, 1)$ multiplets of $SU(2)_L \times SU(2)_R$ for the LH components and in $(1, 2)$ for the RH ones (they are all color triplets and have $Q_X = \frac{1}{6}$). The flavor symmetry forces the localization of the two $(2, 1)$ multiplets to be the same and similarly for the $(1, 2)$ multiplets. The third generation is in an almost custodially protected representation

$$\Psi_l = \begin{pmatrix} t_l[+, +] & X_l[-, +] \\ b_l[+, +] & T_l[-, +] \end{pmatrix} \sim (2, 2), \quad \Psi_r = \begin{pmatrix} X_r[+, -] \\ T_r[+, -] \\ b_r[-, -] \end{pmatrix} \sim (1, 3),$$

$$t_r[-, -] \sim (1, 1). \quad (14)$$

In this case all multiplets have $Q_X = \frac{2}{3}$ and the left and right columns of the bidoublet correspond to fields with $T_R^3 = \mp 1/2$ while the upper and lower components have $T_L^3 = \pm 1/2$. The signs in square brackets are a shorthand for the boundary conditions in the absence of localized brane terms. A Dirichlet boundary condition for the right-handed (RH) component is denoted by $[+]$, whereas $[-]$ denotes a Dirichlet boundary condition for the left-handed (LH) chirality. The first sign corresponds to the boundary condition at the UV brane and the second one at the IR brane.

These boundary conditions are changed on the IR brane due to the presence of the following localized mass terms

$$-\mathcal{S}_{IR} = \int dx^4 \int_R^{R'} dz \left(\frac{R}{z}\right)^4 \delta(z - R') \left\{ M_3 \left[\frac{1}{\sqrt{2}} \psi_{T_r} (\chi_{t_l} + \chi_{T_l}) + \psi_{b_r} \chi_{b_l} + \psi_{X_r} \chi_{X_l} \right] \right. \\ \left. + \frac{M_1}{\sqrt{2}} \psi_{t_r} (\chi_{t_l} - \chi_{T_l}) \right\} + \text{h.c.}, \quad (15)$$

where we denote with χ_Ψ ($\bar{\psi}_\Psi$) the LH (RH) component of field Ψ . These localized masses allow us to give a mass to the third generation of quarks and, as explained in [9], keep $Z b_L \bar{b}_L$ corrections under control.

To check EWPT we canonically normalize the SM gauge fields and obtain, for a fixed value of R' , the parameters R , $g_{5L} = g_{5R}$ and g_{5X} in terms of the measured values of M_W, M_Z and the electromagnetic coupling $e(M_Z)$. We take the PDG's values [20], $M_W = 80.399$ GeV, $M_Z = 91.1876$ GeV and $e(M_Z) = \sqrt{4\pi/128}$. As the first KK gluon mass is given roughly by $m_G R' \sim 2.5$ we choose $R' = 2.5/0.850$ TeV $^{-1}$ obtaining $m_G = 0.848$ TeV. We neglect the mass of the first two generations and work in the zero mode approximation. In that case, choosing $c_L = 0.466$ and $c_R = -0.65$ we obtain the following shifts for the $Z d \bar{d}$ vertex

$$\delta g_{d_R}^Z / g_{d_R}^{Z SM} \sim -0.27\%, \quad \delta g_{d_R}^Z / g_{d_R}^{Z SM} \sim -0.30\%, \quad (16)$$

and similar deviations in the up sector. We consider these values reasonably compatible with EW precision data.² For these values of the bulk masses, the couplings to the KK gluon G are the following

$$g_R^q = -0.26g, \quad g_L^q = 0.19g. \quad (17)$$

Regarding the third generation, for each value of the bulk mass parameters c_{Ψ_L}, c_{Ψ_R} and c_{t_i} , we fix M_1 and M_3 to reproduce the top and bottom masses, $m_t = 170$ GeV and $m_b = 4$ GeV. We find that the top mass cannot be generated, for any value of M_1 and M_3 , unless $c_{\Psi_i} \lesssim 0.35$. Thus, we take $c_{\Psi_i} = 0.35$. We also choose $c_{\Psi_r} = -0.677$ so that the corrections to the $Zb\bar{b}$ vertex that are allowed by EWPT [22]:

$$\delta g_{b_L}^Z / g_{b_L}^{ZSM} \sim -0.08\%, \quad \delta g_{b_R}^Z / g_{b_R}^{ZSM} \sim 2.5\%. \quad (18)$$

Finally, the $Gt_R\bar{t}_R$ coupling is maximized for large values of c_{t_R} although it saturates for $c_{t_R} \gtrsim 1$. We choose $c_{t_R} = 1.6$. With these values of the bulk masses we obtain the following couplings to the first KK gluon G :

$$g_L^t = +1.06g \quad g_R^t = 3.95g \quad (19)$$

$$g_L^b = +1.39g \quad g_R^b = -0.28g. \quad (20)$$

Acknowledgments

We would like to thank J.A. Aguilar-Saavedra and M. Pérez-Victoria and S. Westhoff for useful discussions. This work has been partially supported by MICINN of Spain (FPA2006-05294, FPA2010-16802, FPA2010-17915, Consolider-Ingenio **Multidark** CSD2009-00064 and Ramón y Cajal Program) and by Junta de Andalucía (FQM 101, FQM 3048 and FQM 6552).

References

- [1] V. M. Abazov *et al.* [D0 Collaboration], Phys. Rev. Lett. **100** (2008) 142002. [arXiv:0712.0851 [hep-ex]].
- [2] T. Aaltonen *et al.* [CDF Collaboration], Phys. Rev. Lett. **101** (2008) 202001. [arXiv:0806.2472 [hep-ex]].

²It should be noted that higher dimensional operators could give a non-negligible contribution as could in general be needed to compensate for calculable one loop corrections in these models [21].

- [3] T. Aaltonen *et al.* [CDF Collaboration], [arXiv:1101.0034 [hep-ex]].
- [4] P. Ferrario, G. Rodrigo, Phys. Rev. **D80** (2009) 051701. [arXiv:0906.5541 [hep-ph]].
- [5] O. Antunano, J. H. Kuhn, G. Rodrigo, Phys. Rev. **D77** (2008) 014003. [arXiv:0709.1652 [hep-ph]]; A. Djouadi, G. Moreau, F. Richard, R. K. Singh, Phys. Rev. **D82** (2010) 071702. [arXiv:0906.0604 [hep-ph]]; P. H. Frampton, J. Shu, K. Wang, Phys. Lett. **B683**, 294-297 (2010). [arXiv:0911.2955 [hep-ph]]; Q. -H. Cao, D. McKeen, J. L. Rosner, G. Shaughnessy, C. E. M. Wagner, Phys. Rev. **D81** (2010) 114004. [arXiv:1003.3461 [hep-ph]]; D. Choudhury, R. M. Godbole, S. D. Rindani, P. Saha, [arXiv:1012.4750 [hep-ph]]; Y. Bai, J. L. Hewett, J. Kaplan, T. G. Rizzo, JHEP **1103** (2011) 003. [arXiv:1101.5203 [hep-ph]]; M. I. Gresham, I. -W. Kim, K. M. Zurek, [arXiv:1103.3501 [hep-ph]].
- [6] C. Degrande, J. -M. Gerard, C. Grojean, F. Maltoni, G. Servant, JHEP **1103** (2011) 125. [arXiv:1010.6304 [hep-ph]]; C. Delaunay, O. Gedalia, Y. Hochberg, G. Perez, Y. Soreq, [arXiv:1103.2297 [hep-ph]]; J. A. Aguilar-Saavedra, M. Perez-Victoria, [arXiv:1103.2765 [hep-ph]]; [arXiv:1104.1385 [hep-ph]]; C. Degrande, J. -M. Gerard, C. Grojean, F. Maltoni, G. Servant, [arXiv:1104.1798 [hep-ph]].
- [7] G. Burdman, L. de Lima, R. D. Matheus, Phys. Rev. **D83**, 035012 (2011). [arXiv:1011.6380 [hep-ph]].
- [8] C. Csaki, C. Grojean, H. Murayama, L. Pilo, J. Terning, Phys. Rev. **D69**, 055006 (2004). [hep-ph/0305237]; C. Csaki, C. Grojean, L. Pilo, J. Terning, Phys. Rev. Lett. **92**, 101802 (2004). [hep-ph/0308038].
- [9] G. Cacciapaglia, C. Csaki, G. Marandella, J. Terning, Phys. Rev. **D75** (2007) 015003. [hep-ph/0607146].
- [10] J. Alwall *et al.*, JHEP **0709** (2007) 028 [arXiv:0706.2334 [hep-ph]].
- [11] T. Sjostrand, S. Mrenna and P. Z. Skands, JHEP **0605** (2006) 026 [arXiv:hep-ph/0603175].
- [12] PGS4 <http://www.physics.ucdavis.edu/~conway/research/software/pgs/pgs4-general.htm>
- [13] J. M. Campbell, R. K. Ellis, Phys. Rev. **D60**, 113006 (1999). [hep-ph/9905386].
- [14] M. Bauer, F. Goertz, U. Haisch, T. Pfoh, S. Westhoff, JHEP **1011** (2010) 039. [arXiv:1008.0742 [hep-ph]].

- [15] C. Csaki, D. Curtin, Phys. Rev. **D80** (2009) 015027. [arXiv:0904.2137 [hep-ph]].
- [16] R. S. Chivukula, E. H. Simmons, C. -P. Yuan, Phys. Rev. **D82** (2010) 094009. [arXiv:1007.0260 [hep-ph]].
- [17] CMS Collaboration, public note CMS PAS TOP-10-007.
- [18] G. Aad *et al.* [ATLAS Collaboration], [arXiv:1103.3864 [hep-ex]].
- [19] M. Carena, A. D. Medina, B. Panes, N. R. Shah, C. E. M. Wagner, Phys. Rev. **D77** (2008) 076003. [arXiv:0712.0095 [hep-ph]].
- [20] K. Nakamura *et al.* [Particle Data Group Collaboration], J. Phys. G **G37** (2010) 075021.
- [21] S. Matsuzaki, R. S. Chivukula, E. H. Simmons, M. Tanabashi, Phys. Rev. **D75**, 073002 (2007). [hep-ph/0607191]; R. S. Chivukula, E. H. Simmons, S. Matsuzaki, M. Tanabashi, Phys. Rev. **D75**, 075012 (2007). [hep-ph/0702218 [HEP-PH]]; S. Dawson, C. B. Jackson, Phys. Rev. **D76**, 015014 (2007). [hep-ph/0703299 [HEP-PH]]; Phys. Rev. **D79**, 013006 (2009). [arXiv:0810.5068 [hep-ph]]; T. Abe, R. S. Chivukula, N. D. Christensen, K. Hsieh, S. Matsuzaki, E. H. Simmons, M. Tanabashi, Phys. Rev. **D79**, 075016 (2009). [arXiv:0902.3910 [hep-ph]].
- [22] D. Choudhury, T. M. P. Tait, C. E. M. Wagner, Phys. Rev. **D65** (2002) 053002. [hep-ph/0109097].